International Journal of Advanced Research in Chemical Science (IJARCS)
Volume 1, Issue 5, July 2014, PP 17-29
ISSN 2349-039X (Print) & ISSN 2349-0403 (Online)
www.arcjournals.org

Evaluation of Kinetic and Thermodynamic Parameters of Chromium Adsorption on a Organobentonite

[1]My. S. Slimani, [2]H. Ahlafi, [3]H. Moussout, [4]R. Chfaira, [5]O. Zegaoui

Laboratory of Chemistry and Biology Applied to the Environment,
Faculty of Sciences,
My Ismail University, BP -Zitoune,
Meknès, Morocco
[1]slimanimyslimane@gmail.com, [2]hahlafi@yahoo.fr, [3]moussouthammou@gmail.com
[4]chfaira65@gmail.com, [5]zomar17@yahoo.fr

Abstract: *Bentonite (Bt) and the prepared hexadecyltrimethylammonium bromide bentonite (HDTMABt) were used to remove Cr(VI) from aqueous solutions. Characterization of these materials by X-ray diffraction (XRD), Fourier Transform Infrared (FTIR) spectroscopy, GTA/DTA and surface area (BET) measurements demonstrated that the $HDTMA^+$ polymer was intercalated in the interlayer space of Bt. The electrochemical studies revealed that the pH of point of zero charge (pH_{pzc}) was close to pH = 10. Batch experiments indicated that the adsorption process proceeds kinetically according to pseudo-second-order model. The Langmuir and Freundlich adsorption isotherms provided the best correlation of the equilibrium data for both sample. HDTMA/Bt adsorbent showed a maximum efficiency, exhibiting a better adsorption capacity for Cr(VI) than Bt at pH = 2. Thermodynamic parameters including the Gibbs free energy ($\Delta G°$), enthalpy ($\Delta H°$), and entropy ($\Delta S°$), were also calculated. These parameters indicated that adsorption of Cr (VI) onto HDTAM-bentonite was feasible, spontaneous and endothermic.*

Keywords: *Adsorption, chromium, isotherm, organobentonite, conductometric titrations.*

1. INTRODUCTION

The heavy metal contamination is a serious problem to the environment, because the anthropogenic activities from mining, processing and applications of these metals have increased enormously during the past few decades. Hence their removal/remediation has become all the more necessary. Over a few years, the discarding solid and/or liquid waste products containing heavy metals emanating from the industrial processes has received a lot of attention, and consequently legislation for the protection of the environment has gradually become more rigid [1].

Chromium(VI) is known to be very toxic heavy metal and a common element of earth's [2]. Chromium acts as carcinogens, mutagens, and teratogens in biological systems. It can enter the environment through surface waters and even reach groundwater in a number of path ways. These include discharge of wastewater from industries such as those of electroplating and leather tanning. According to the guidelines recommended by the World Health Organization (WHO), the maximum level for Cr(VI) in drinking water is 0.05 mg L[3]. Accordingly, chromium containing wastewaters must be treated to lower the Cr (VI) to permissible limits prior to discharge.

Several treatment technologies have been reported for the removal of chromium from aqueous solutions and effluents. For example, chemical precipitation [4], nanofiltration [5], membrane [6], ion exchange [7] and adsorption process [8]. Among them, adsorption is one of the most promising techniques for heavy metals removal, on account of its advantages of easy operation and low cost when the adsorbent is efficient and cheaper like clay or other natural adsorbents [9, 10]. Clay materials can also be modified with organic surfactants using a variety of chemical/physical treatments to achieve the desired surface properties for best immobilization of organic and inorganic pollutants [11]. The organic modifiers used for this purpose are generally

cationic quaternary amine compounds and have also been reported to be good adsorbent materials [12]. Krishna et al. [13], reported improved adsorption of chromate oxyanion by HDTMA modified kaolinite, montmorillonite and pillared montmorillonite as compared to the unmodified clays. The authors found that the amount of adsorption decreased with increasing pH of the solution.

The aim of this article is to complement the previous study on the adsorption capacity of chromium on a modified commercial bentonite by Hexadecyltrimethylammonium bromide (HDTMABt) [14]. Adsorption isotherm, kinetic and thermodynamic parameters have been estimated from experimental results. Original method based on the conductometric titration to determine the pzc of Bt was developed**.**

2. MATERIALS AND METHODS

2.1. Materials

The bentonite (Bt) was provided from Rhone Poulenc Company (France). All other reagents such as $AgNO_3$, HDTMABr, Potassium dichromate ($K_2Cr_2O_7$), NaCl, CsCl, NaF, NaF, LiCl, HCl and NaOH were purchased from Aldrich chemicals and specified to be ≥ 99% purity. Deionised water was used in all experiments.

2.2. Preparation of HDTMABt Composite

Prior to the HDTMABt preparation, the Bt was treated by NaCl to form sodium bentonite (NaBt). The latter was prepared by stirring a known amount of Bt in 200 ml of 10^{-1} mol/L NaCl solution during 24h at room temperature, then it was separated by centrifugation (15000 rpm) and washed several times until no Cl is was detected by $AgNO_3$ test. The composite HDTMABt was prepared by exchanging Na^+ in NaBt by $HDTMA^+$ cations as follows: a total amount of 30 g of NaBt was added to the known concentration of surfactant solution (10^{-1} M) and stirred for 24 h with a mechanical stirrer at 25 °C. The composite was separated from the solution by centrifugation, and the excess of the surfactant was removed by repetitive washing with distilled water. The obtained HDTMABt was dried in air at 60 °C, ground and stored.

2.3. Batch Adsorption Experiments

Adsorption of chromium (VI) on Bt and HDTMABt adsorbents was performed in batch experiments. Initial concentrations of chromium ranged between 6.10^{-5}M - 8.10^{-3} M were used. A mass of 0.2 g of adsorbents were mixed with V = 20 mL of chromium solutions in erlenmeyer flasks with glass caps. The samples were mixed by magnetic stirring at 150 rpm shaken for different times of adsorption (t_{ads}) at certain temperature (T_{ads}). The pH solutions were adjusted by adding negligible volumes of 0.1mol/L HCl or NaOH. After a given t_{ads}, the solid and liquid phases were separated by centrifugation at 15000 rpm. The residual concentration of chromium in supernatant were measured by UV/Visible spectrophotometer (UV/Vis 2100 from Shimadzu) at λ = 350 nm. The amount of chromium adsorbed at equilibrium on Bt or HDTMABt was calculated using the following equation:

$$q_e = \left(\frac{C_0 - C_e}{m} \right).V$$

Where C_0 and Ce were the initial and the equilibrium concentrations of pollutants (mg/L), respectively, m was the mass of adsorbent (g) and V the volume of the solution (L).

2.4. Characterizations of Materials

Several spectroscopic techniques were used to characterize Bt and HDTMABt samples before and after adsorption of pollutants: (a) XRD patterns were obtained using a X'PERT MPD-PRO wide angle X-ray powder diffractometer operating at 45 kV and 40 mA with CuKλ radiation, (b) FTIR spectra were recorded in absorption frequencies (400 – 4000 cm^{-1}) in an FTIR (Shimadzu, JASCO 4100). The samples were prepared in KBr discs from very well dried mixtures of about

4% (w/w) and stored in a desiccator, (c) N_2 adsorption measurements at - 196 °C were performed using an ASAP 2010. The specific surface area and the average pore diameter were determined according to the standard BET and BJH (Barrett, Joyner and Halenda) methods, respectively and (d) the dynamic degradation studies for the samples were carried out in air atmosphere in a TA60 SHIMADZU thermal analyzer simultaneous TGA-DTA. For the dynamic experiments the samples were heated from ambient to 600°C at the heating rate β = 20°C/min.

2.5. Principle of Determining the Surface Charge Density

The surface charge density of Bt studied, results from the uneven ions adsorption, which determine the potential H^+ and OH^- [1]. The experimental measures of this charge were obtained by the potentiometric titrations of the solid suspensions in the presence of a known constant concentration of the electrolyte used [33]. The experimental determination of the pzc of a colloidal suspension can be made by several methods. The most widely used experimental approach is the one which, independently of the concentration of the salt, if volumetric potentiometric titrations are realized according to pH and to the concentration of salt, these curves cross at a unique point which is the point of zero charge. As for metallic oxides the surface charge results from the unequal adsorption ions determining the potential, H^+ and OH^-, so this method consists to determine the state of ions were consummated by various sites of surface.

3. RESULTS AND DISCUSSION

3.1. Characterization of Bt and HDTMABt

The FTIR spectra of the unmodified Bt and its modified forms (HDTMABt) are presented in fig.1. In the OH region, between 3100 cm^{-1} and 3700 cm^{-1}, two bands can be distinguished at 3625 and 3425 cm^{-1} accompanied by a shoulder at 3220 cm^{-1}. The latter was attributed to the water hydrogen bonded to other water molecules within the interlayer [15]; whereas the first band at 3625 cm^{-1} was attributed to the inner OH unit within the clay structure. The characteristic bands in the region 900–1200 cm^{-1} are attributed to different types of Si–O and Si–O–Si stretching vibrations. Additional bands between 450 and 900 cm^{-1} in the spectrum of Bt were assigned to typical Si–O and Si–O–Al bending modes [16]. It can be noted the appearance of new bands located at 2850 cm^{-1} and 2925 cm^{-1} in the spectrum of HDTMABt sample. These bands are related to the symmetric and asymmetric stretching vibration of CH_2 and CH_3 which give two bending vibrations located at 1463 and 1480 cm^{-1} due to the methylene scissoring modes.The presence of these C-H vibrations suggested that the composition of the modified Bt in the interlayer space may have resulted from ion exchange of Na with the quaternary ammonium cation [16, 17]. It's also observed (fig.1) that the band at 3425 cm^{-1}, which was originated from adsorbed water, shifts to lower frequency from 3460 cm^{-1} to 3425 cm^{-1} accompanied with a decrease in their absorbance. These modifications can be linked to the interaction of $HDTMA^+$ in the interlayer of Bt with OH groups. Similar results were reported by other authors using bentonite or other clays [18].

Fig.2 shows the XRD patterns of Bt and HDTMABt samples. For Bt, the basal spacing d(001) centered at 2θ° = 5.7 was shifted to 2θ° = 4.5 in the HDTMABt indicating that the $HDTMA^+$ cations have been intercalated within the layered structure widened the basal spacing d(001) of Bt. The new peaks appearing at 2θ° = 3.6 and 2θ° = 6.9 are attributed to organic cations associating predominantly flat with the silicate surface in an inclined paraffin-type structure via cation exchange of interlayer (Na+/ $HDTMA^+$) of [19]. The new peaks appearing in the HDTMABt spectrum were attributed to the intercalated $HDTMA^+$ polymer.

The above results explain the decrease in BET specific surface area and cumulative pore volume when Bt was modified by $HDTMA^+$ and the increase of the average pore diameter. The surface area of Bt and HDTMABt composite were found to be 19.43 and 2.04 m^2/g, respectively, due to the good intercalation of the $HDTMA^+$ cations within the interlayer space of Bt, as a result, enhanced their inaccessibility for nitrogen adsorption [20].

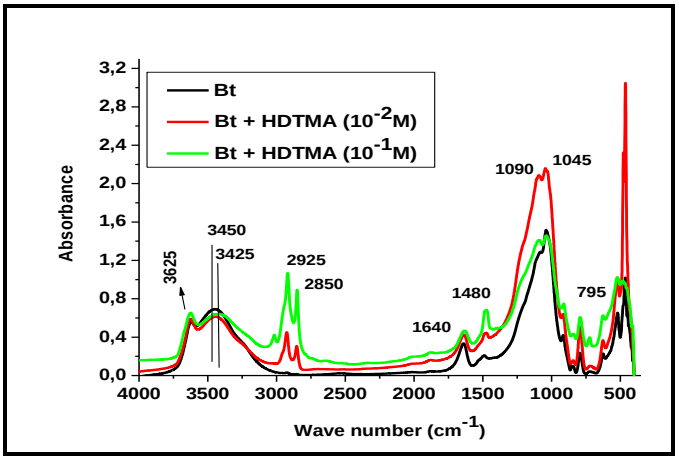

Fig 1. *FTIR spectra of Bt and HDTAMBt*

Thermal analysis using thermogravimetric (TG) techniques enables the mass loss steps and the mechanism for the mass loss to be determined. The TG analysis curve related to Bt and HDTMABt exhibited mass losses by 8.225% and 55.02% respectively, in temperature ranges 25–600°C (Fig.3). Differential thermogravimetric (DTG) analysis of these samples were also illustrated in Fig.3, to observe the modifications occurred. The intensity of the DTG peaks located at 253 and 400°C for HDTMABt which are not observed in the DTG curve of Bt are due to the degradation steps of $HDTMA^+$ and consequently, they confirm the bonding of the surfactant with Bt. The change in mass involved in the first step at 77°C for Bt (-8.225%) was attributed to the removal of physically adsorbed water. The mass loss corresponding to this peak was further reduced to 1.67% in the TG curve of HDTMABt, confirming the exchange reaction between $HDTMA^+$ and the exchangeable water $^+$ in the interlayer space of Bt.

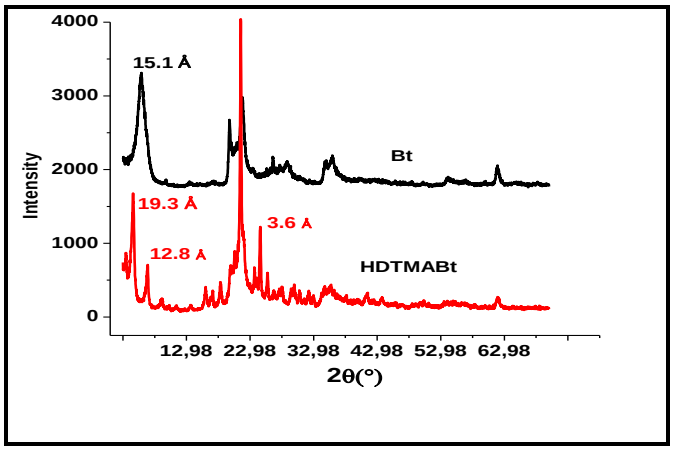

Fig 2. *XRD paterns of the Bt and HDTAMBt*

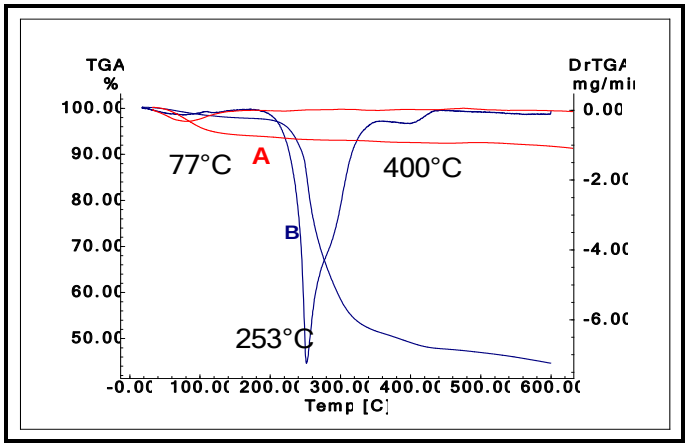

Fig.3. *TGA and DTGA curves for Bt and $HDTMA^+$ intercalated bentonite*

3.2. Electrochemical Properties of the Interface Bt/Dispersing Phase

3.2.1. The Point of Zero Charge: pzc

In principle, in absence of specific adsorption, the net point of zero charge corresponds to the intersection of the isotherms of charge adsorption of measured surface at various ionic forces. Figure 4A shows the variation of surface charge density of Bt according to the pH and to the ionic strength of the electrolyte NaCl. We clearly notice, that these surface charge curves cross at a unique point which is the pH at the pzc. For Bt in the presence of a non specifically adsorbed electrolyte such as CsCl, NaCl or NaBr, the measured value of the pH_{pzc} is 10±0,1. In pH above this point, the studied solid nanoparticles are negatively charged while at pH less than the pH_{pzc}, the nanoparticles are positively charged.

The exploitation of the curves of the conductometric titrations in absence and in presence of the solid, led us to develop an original method for the determination of the point of zero charge of a colloidal suspension. Figure 4B shows the application of this new technique in the case of Bt in the presence of NaCl electrolyte. We can see that the curve $\Delta\chi$ ($\Delta\chi = \chi_{white} - \chi_{solide}$), according to the measured pH on different ionic strengths, takes a form that is constituted of two branches with the tangents cross at a unique point which is the pH_{pzc}. The found value is in the order of 9.9±0,1 which is similar to the value measured with the potentiometric titrations technique.

3.2.2. Total Number of Surface Sites: Ns

Ns was determined by extrapolation technique introduced by Stumm, Huang and Jenkins's [21, 22]. It's based on the choice of the electrolytes which depends on the nature of the solid action on the dispersing phase. Thus, for the organizing oxides of the structure of the water, as the case of the studied Bt, it is necessary to choose for the positive surface of the solid, the graphic extrapolation of the curve ($1/[H_s^+]$) vs ($1/\sigma_O$) corresponding to the most electronegative anion, F^-, which is the most organizing and most adsorbed. For the negative surface of the solid, it is necessary to choose the graphic extrapolation of the curve $[H_s^+]$ vs ($-1/\sigma_O$) corresponding to the most electropositive alkaline cation Li^+ which is the most adsorbed.

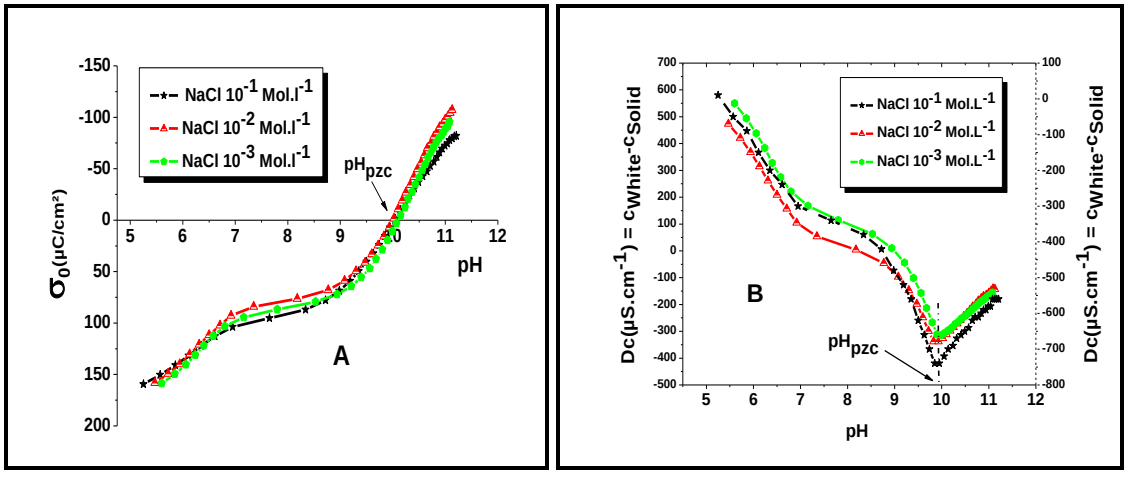

Fig 4. *Determination of the pH_{pzc} for Bt by potentiometric (A) and conductometric (B) titrations*

The graphic extrapolation corresponding to the anion F^- allows determining the number of positive sites N_s^+ and the one corresponding to the ion Li^+ gives the number of negative sites N_s^-. The total number of sites is $N_s = N_s^+ + N_s^-$. The total density of surface sites for the disorganizing oxides is opposite to that of the organizing surfaces.

Figures 5A and 5B shows the obtained straights and their corresponding equations respectively in the adsorption of the ion F^- and the ion Li^+. The calculated value of N_s^+ is to be 123.04 µC/cm^2 and that of N_s^- is in the order of 121.42 µC/cm^2. The total density of surfaces sites (Ns) of Bt is: $N_s = N_s^+ + N_s^-$ = 244.46 µC/cm^2. This value does not exactly translate the maximal exchange

capacity adsorbat-adsorbing of the Bt. It is necessary to convert Ns in number of OH group/nm^2, called sites density by unit of surface, and noted Ds.

$$D_S = \frac{\text{numbreof surfacesites}}{\text{unitof surface}} = \frac{n_S \cdot N_{Av}}{A \cdot m_S} = 6{,}24.10^{-2}.Ns \ \ OH/nm^2 = 15.25 \cong 16 \ OH/nm^2$$

Where A is the solid specific surface area of Bt, m_s is the mass of Bt, n_s is the equivalent number of mole of titrated sites and N_{Av} is the Avogadro number.

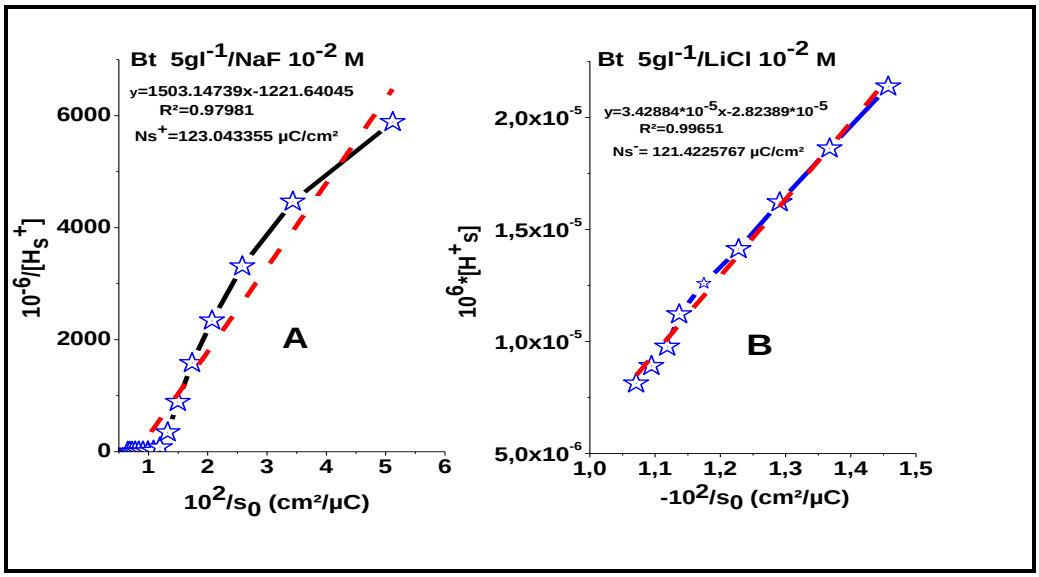

Fig 5. *Determination of the total density of surface sites Ns for Bt*

3.3. Sorption Kinetics: Effect of Contact Time

For kinetic study, 2.10^{-4}M hexavalent chromium solutions (V = 20 mL, pH = 2) were stirred with 0.2g of each adsorbent at room temperature and at different time of adsorption. The experimental data (fig.6) indicated that the adsorption of chromium was very fast at the beginning and then approached equilibrium after only 15 min for HDTMABt and 45 min for Bt. The adsorption capacity of chromium is found to be 2.5 and 251.7 mg/g for Bt and HDTAMBt respectively. The higher value of adsorption capacity of chromium on modified bentonite is essentially linked to its adsorption on HDTMABt surface.

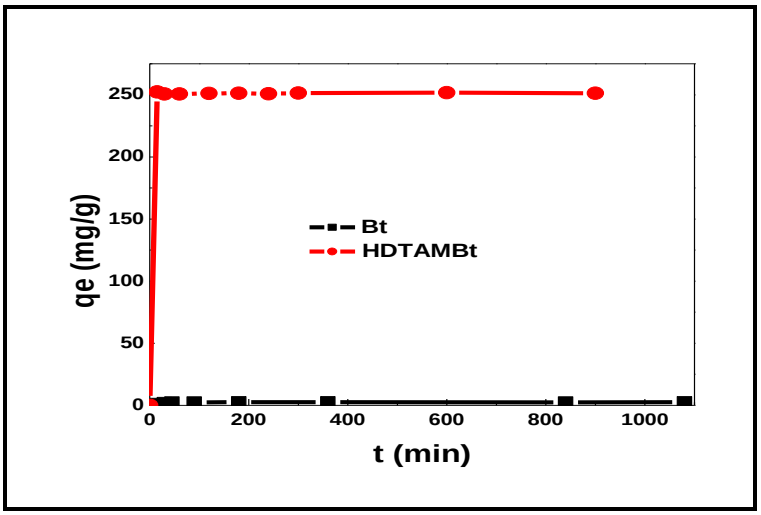

Fig 6. *Chromium adsorption on Bt and HDTAMABt as a function of contact time*

In order to examine the adsorption mechanism such as mass transfer and chemical reaction, the kinetic data were fitted with the linear forms of equations, which have been used to model the kinetic parameters for pseudo-first-order, pseudo-second-order and intra-particle diffusion:

- Pseudo-first order model: $\log(q_e - q_t) = \log q_e - \frac{K_1}{2.303} t$

- Pseudo-second order model: $\frac{t}{q_t} = \frac{1}{K_2 \cdot q_e^2} - \frac{1}{q_e} t$

- Intra-particle diffusion: $q_t = K_d t^{0.5} + C$

Where k_1 (min^{-1}) and k_2 (g/mg.min) are rate constants of adsorption, qe(mg/g) is the equilibrium adsorption capacity, qt is the adsorption at any time t (min) and Kd is the intra-particle diffusion constant (mg/g $min^{0.5}$) and C is a constant.

The rate constants and regression coefficients of these models were calculated to determine the best fitted model (Table 1). The regression coefficients and the values of qe demonstrated that the pseudo second order model fitted the experimental data better than the other two kinetic models. The calculated $q_{e\ calc}$ value is closer to the experimental $q_{e\ exp}$ value.

In the other hand if the adsorption process follows the intraparticle diffusion model, a plot of qe against $t^{0.5}$ may present a multi linearity indicating that two or more steps take place. Fig. 7 (A) and (B), indicate that for Bt two steps occurred in the adsorption process while in the case of HDTAMABt only one straight line was obtained. These results imply that the kinetic of the removal of Cr onto these samples are different. The linear processes as well as their deviation from the origin suggest that the intraparticle diffusion is involved but it is not the rate controlling step during the adsorption of chromium onto Bt and HDTAM-Bt. The intraparticle diffusion parameters and the determination coefficients were summarized in Table 2. For Bt the first sharper section (Fig 7(A)) is the external surface adsorption or instantaneous adsorption stage. The second subdued portion is the gradual adsorption stage, where intraparticle diffusion is rate-controlled [23].

Table 1. *Kinetics parameters for pseudo- first order, pseudo-second order and intra-particle diffusion*

	Pseudo-first order				Pseudo-second order			Intraparticle diffusion			
Sample	qe (exp) mg/g	qe (calc) mg/g	K_1 min^{-1}	R^2	qe (calc) mg/g	K_2 g/mg.min	R^2	Kd_1 mg/g $min^{0.5}$	R^2	Kd_2 mg/g $min^{0.5}$	R_2
Bt	2.5	1.16	0.008	O.995	2.5	$8.65.10^{-2}$	0.999	0.474	0.999	-	0.02
HDTMABt	251.7	5.75	4.10^{-5}	0.996	270.3	0.006	0.999	0.005	0.999	-	-

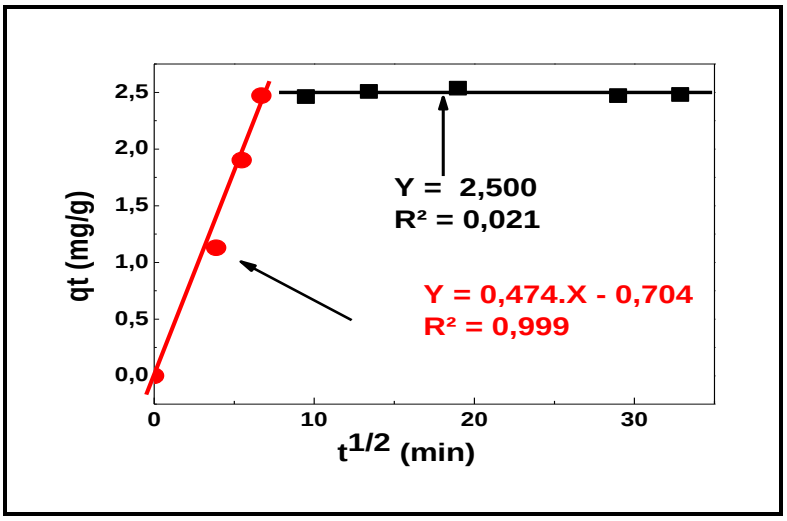

Fig 7(A). *Intraparticle diffusion models for Cr(VI) adsorption onto Bt*

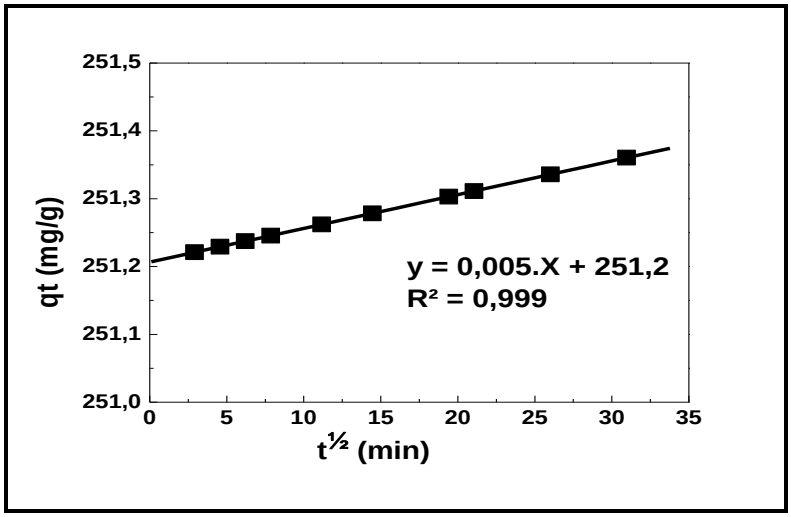

Fig 7(B). *Intraparticle diffusion models for Cr (VI) adsorption onto HDTAMBt*

3.4. Equilibrium Isotherms

In order to optimize the design of an adsorption system, it is important to establish the most appropriate correlation for the equilibrium data. Many models have been proposed to explain adsorption equilibrium; however, the important factor is to have applicability over the entire range of process conditions. In this study, two adsorption isotherms: Langmuir and Freundlich models were applied to fit the equilibrium data of adsorption of Cr(VI) onto Bt and HDTAMBt. The linear equation of the Freundlich adsorption model is expressed by:

$$\log(q_e) = \log(K_f) + \frac{1}{n}\log C_e$$

Where K_F and 1/n are the Freundlich constants, and the linear equation of the Langmuir adsorption model is expressed by:

$$\frac{C_e}{q_e} = \frac{1}{q_m.K_L} + \frac{C_e}{q_m}$$

Where qm (mg/g) is the maximum adsorption capacity and K_L is the binding constant which is relate to the heat of adsorption. The favorable nature of adsorption can be expressed in terms of the separation factor, R_L, defined as:

$$R_L = \frac{1}{1 + K_L.C_0}$$

The parameter R_L can be used to predict the affinity between the adsorbent and the adsorbate according to the criteria: not favorable for $R_L > 1$, linear for $R_L = 1$, favorable for $0 < R_L < 1$, and irreversible for $R_L = 0$.

The linearized Freundlich and Langmuir plots are given in Figs 8(A) and (B), respectively. These linearized plots were used to calculate the adsorption constants tabulated in Table 3. From Table 3, higher correlation coefficients indicate that the Langmuir model fits the adsorption data better than the Freundlich model for Bt sample and inversely in the case of HDTMABt. All values of R_L calculed for Bt and HDTAMBt vary between 0 and 1 indicating that adsorption is favorable for both adsorbents. In addition the Freundlich constant (1/n) for Bt and HDTMABt are smaller than 1, which is indicative of high adsorption affinity between adsorbent and adsorbate.

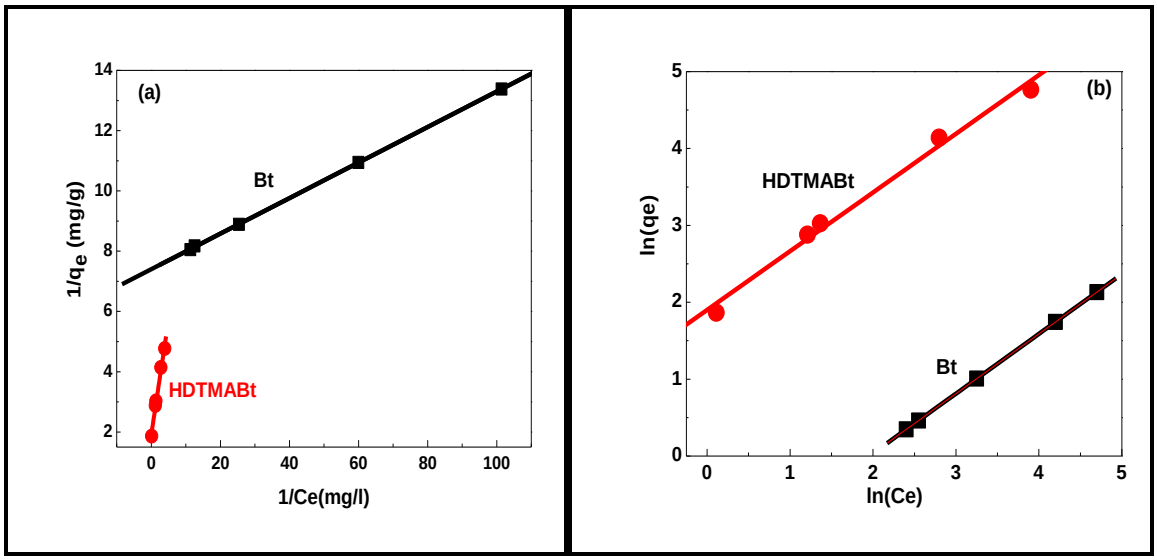

Fig 8. *Langmuir (A) and Freundlich (B) isotherms plot for chromium adsorption*

Table 2. *Model Isotherm constants for chromium adsorption onto Bt and HDTMABt*

Adsorbent	Langmuir				Freundlich		
	q_{max} (mg/g)	K_L	R^2	R_L	K_F	1/n	R^2
Bt	16.95	$7.97.10^{-3}$	1	0.415	0.22	0.777	0.995
HDTAMBt	250	0.024	0.995	0.414	6.68	0.763	1

3.5. Thermodynamics

The feasibility of the adsorption process was evaluated by the thermodynamic parameters including free energy change (Δ*G*°), enthalpy change (Δ*H*°), and entropy change (Δ*S*°). Δ*G*° was calculated from the following equations:

$$\Delta G° = -RT\ln Kc$$

Where R is the universal gas constant ($kJmol^{-1}\ K^{-1}$), T is the temperature (K), and K_c is the distribution coefficient defined by:

$$K_c = \frac{q_e}{C_e}$$

The Gibbs free energy change is also related to enthalpy change (ΔH°) and entropy change (ΔS°) at constant temperature by the following equation:

$$\ln Kc = \frac{\Delta S°}{R} - \frac{\Delta H°}{R.T}$$

The values of (ΔH°) and (ΔS°) were calculated from the slope and the intercept of Van't Hoff plot ($\ln K_c$ vs. 1/T) shown in fig.9. Table 3 shows the negative values of ΔG° which indicated the feasibility and spontaneity of Cr (VI) adsorption onto the two samples. The enthalpy change (ΔH°) values were found to be positive and less than 40 kJ/mol, which indicated the endothermic and physisorption nature of adsorption process [23]. The decrease in ΔG° with the increase of temperature indicated more efficient adsorption at higher temperature. The negative value of ΔS°

suggested the decreased randomness at the solid/liquid interface during the adsorption of chromium onto Bt and HDTAMBt [24, 25].

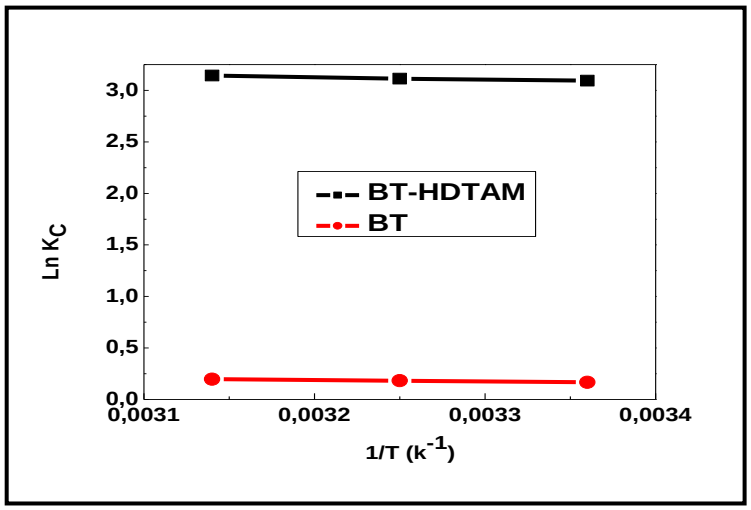

Fig 9. *Van't Hoff plot for estimation of thermodynamic parameters*

Table 3. *Thermodynamic parameters for chromium adsorption onto Bt and HDTAMBt*

Adsorbent	T(K)	ΔG° (kJ.mol^{-1})	ΔS° (kJ.mol^{-1}.K^{-1})	ΔH° (kJ.mol^{-1})	R^2
Bt	298	- 0,42	0.0055	1.177	1
	308	-0.47			
	318	-0.52			
HDTMABt	298	-7.56	0.0333	1.863	0.982
	308	-7.72			
	318	-8.21			

In order to understand the difference between the observed adsorption data, obtained for chromium, it is important to take into account the experimental conditions applied for chromium adsorption, in particular the pH value which influence strongly the adsorption onto the solid/liquid interface. Some researchers [26,27] have recently shown in their evaluation of modified mineral performance for chromium sorption from aqueous solutions that the high adsorption capacity of $HDTMA^+$-clay has shown a maximum at pH = 3-4 and has been linked to the adsorption of predominate $HCrO4^-$ and $Cr_2O_7^{2-}$ species of Cr(VI). Thus, at pH = 2 the negatively charged chromium species interact with the intercalated $HDTMA^+$ cations which enhances, therefore, the adsorption of chromium species. This may be due to electrostatic attraction forces working between the organoclay and $HCrO_4^-$ and $Cr_2O_7^{2-}$ [28, 29]. Majdan et al. [30] observed an 11.5 Å increase in d(001) basal spacing value on the SWAXS (Small wide angle X-ray scattering measurements) pattern recorded before and after adsorption of chromium. This shifts was attributed to the presence of dichromates $(HDTMA)_2Cr_2O_7$ and chromates $(HDTMA)(HCrO_4)$ in the interlayer space of HDTMA-bentonite. For XRD pattern of chitosan clay composite, the new peaks observed after adsorption of Cr(VI) at pH = 3 and the shifts of d(001) to lower 2θ°, were linked to the adsorbed Cr(VI) onto the silicate surface and also in the lamellar space of the cloisite 10 Å [31]. In this study, the FTIR spetrum shown in Fig.12 was recorded after the adsorption of Cr(VI) on HDTMABt. Compared to the spectrum of HDTMABt, we can noted that all the frequency shifted, especially for the bands corresponding to (-OH: 3620 cm^{-1}), (-CH_2: 2925 and 2860 cm^{-1}), Si-O: 1090 cm^{-1}), which reflect the interaction of chromium species with these groups at the surface and in the interlayer space of HDTMABt via an electrostatic force of attraction [32].

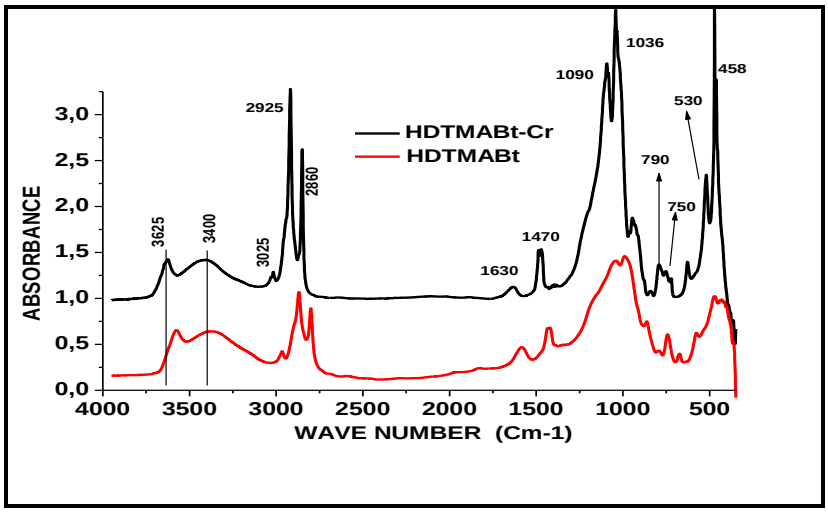

Fig 12. *spectra of HDTAMBt and adsorbed chromuim*

4. CONCLUSIONS

The intercalation of $HDTMA^+$ cations within the interlayer space were confirmed using various useful techniques. The experiments showed that the organoclay with higher surfactant concentration ($C=10^{-1}$ M) was more effective in removing chromium species pollutants than the original Bt exchanged bentonite. The maximum chromium uptakes were achieved at pH = 2. The kinetic studies indicated that the adsorption process was extremely fast on HDTMABt, and the sorption system fitted well with pseudo-second order for chromuim. For the adsorption of chromium the experimental isotherms were best described by Freundlich and Langmuir models. The calculated variation of the free energy (ΔG°) and enthalpy (ΔH°) indicated that the adsorption process was spontaneous and endothermic in nature for chromium. The results of this study indicate that HDTMABt was an effective sorbent for chromium.

REFERENCES

[1] A. Benedetti, Defining soil quality: introduction to round table, in: S. de Bertoldi, F. Pinzari (Eds.), COST Actions 831, Joint WCs Meeting, Biotechnology of soil: monitoring conservation and remediation, 1998, pp 29–33.

[2] R. Rakhunde, L. Deshpande, H.D. Juneja, Chemical speciation of chromium in water: a review, Critical Rev. Environ. Sci. Technol. 42 (7) (2012),776–810.

[3] M. Bhaumik,A.Maity,V.V.Srinivasu,M.S.Onyango,Enhanced removal of Cr(VI) from aqueous solution using polypyrrole/Fe 3O4 magnetic nanocomposite, J.Hazard.Mater.190 (2011), 381–390.

[4] V.K. Gupta, I. Ali, T.A. Saleh, A. Nayak, S. Agarwal, Chemical treatment technologies for waste-water recycling – an overview, RSC. Adv. 2 (2012), 6380–6388.

[5] M.J. Gonzalez-Munoz, M. Amparo Rodriguez, S. Luque, J. Ramon Alvarez, Recovery of heavy metals from metal industry waste waters by chemical precipitation and nanofiltration, Desalination 200 (2006), 742–744.

[6] L. Yu, R. Zou, Z. Zhang, G. Song, Z. Chen, J. Yang, J. Hu, A Zn2 GeO4-ethylenediamine hybrid nanoribbon membrane as a recyclable adsorbent for the highly efficient removal of heavy metals from contaminated water, Chem. Commun. 47 (2011), 10719–10721.

[7] H.A. Maturana, I.M. Peric, B.L. Rivas, S.A. Pooley, Interaction of heavy metal ions with an ion exchange resin obtained from a natural polyelectrolyte, Polym. Bull. 67 (2011), 669–676.

[8] L. Ravikumar, S.S. Kalaivani, A. Murugesan, T. Vidhyadevi, G. Karthik, S.D. Kirupha, S. Sivanesan, Synthesis, characterization, and heavy metal ion adsorption studies of polyamides, polythioamides having pendent chlorobenzylidine rings, J. Appl. Polym. Sci. 122 (2011), 1634–1642.

[9] G. Zhang, Z. He, W. Xu, A low-cost and high efficient zirconium-modified-Naattapulgite adsorbent for fluoride removal from aqueous solutions, Chem. Eng. J. 183 (2012), 315–324.

[10] U. Yildiz, O.F. Kemik, B. Hazer, The removal of heavy metal ions from aqueous solutions by novel pH-sensitive hydrogels, J. Hazard. Mater. 183 (2010), 521– 532.

[11] Q. Zhou, H. He, R.L. Frost, Y. Xi, Adsorption of p-nitrophenol on mono-, di-, and trialkyl surfactant-intercalated organoclays: a comparative study, J. Phys. Chem. C111 (2007), 7487–7493.

[12] P. C, K. Litina, D. Gournis, T.S. Giannopoulos, Y. Deligiannakis, Physicochemical study of novel organoclays as heavy metal ion adsorbents for environmental remediation, J. Colloid Interface Sci. 316 (2007), 298–309.

[13] B.S. Krishna, D.S.R. Murty, B.S. Jai Prakash, Surfactant-modified clay as adsorbent for chromate, Appl. Clay Sci. 20 (2001), 65–71.

[14] My. S. Slimani, H. Ahlafi, H. Moussout, F. Boukhlifi, O. Zegaoui, Adsorption of Hexavalent Chromium and phenol onto Bentonite Modified With HexaDecylTriMethylAmmonium Bromide (HDTMABr), Journal of Advances in Chemistry. Vol. 8, No. 2, (2014).

[15] W., Xue, H., He, J., Zhu, P.,Yuan, FTIR investigation of CTAB–Al–montmorillonite complexes. Spectrochimica Acta Part A 67, (2007), 1030–1036.

[16] Z., Li, W.T., Jiang, H., Hong, An FTIR investigation of hexadecyltrimethylammonium intercalation into rectorite. Spectrochimica Acta Part A 71, (2008), 1525–1534.

[17] Z., Hu, G., He, Y., Liu, C., Dong, X., Wu, W., Zhao, Effects of surfactant concentration on alkyl chain arrangements in dry and swollen organic montmorillonite. Applied Clay Science, 75–76, (2013), 134–140.

[18] V.N., Nguyen, T.D.C, Nguyen, T.P., Dao, H.T., Tran, D.B., Nguyen, D.H., Ahn, Synthesis of organoclays and their application for the adsorption of phenolic compounds from aqueous solution. Journal of Industrial and Engineering Chemistry 19, (2013), 640–644.

[19] B.,Sarkar, Y.,Xia, M.,Megharaj, G.S.R., Krishnamurtia, D., Rajarathnam, B.,Naidu, Remediation of hexavalent chromium through adsorption by bentonite based Arquad® 2HT-75 organoclays. Journal of Hazardous Materials 183, (2010), 87–97.

[20] K.S.W. Sing, D.H. Everett, R.A.W. Haul, L. Moscou, R.A. Pierotti, J. Rouquerol, T.Siemieniewska, Pure Appl. Chem. 57 (1985) 603–619.

[21] W.,Stumm, Chemistry of the solid-water interface: Processes at the mineral-water and particle-water interface in natural system ; Wiley Interscience Pub., New York 1992.

[22] C.-P., Huang and W. Stumm, J. Coll. Inter. Sci., 43, (1973), 409-420.

[23] L.A. Rodrigues et al. / Journal of Hazardous Materials 173 (2010), 630–636.

[24] F.S., Maather, J.R. Peralta-Videa , J.R.,Gonzalez , M.D.,Gardea, J.L. Gardea-Torresdey, Thermodynamic and isotherm studies of the biosorption of Cu(II), Pb(II), and Zn(II) by leaves of saltbush (Atriplex canescens), J. Chem. Thermodynamics, 39 (2007),488–492.

[25] Mehmet Emin Argun , Sukru Dursun, Celalettin Ozdemir, Mustafa Karatas, Heavy metal adsorption by modified oak sawdust:Thermodynamics and kinetics, Journal of Hazardous Materials, 141 (2007), 77–85.

[26] Z., Hu, G., He, Liu, Y., C., Dong, X., Wu, W., Zhao, Effects of surfactant concentration on alkyl chain arrangements in dry and swollen organic montmorillonite. Applied Clay Science, 75–76, (2013), 134–140.

[27] A.G.,Thanos, E.,Katsou, S.,Malamis, K.,Psarras, E.A.,Pavlatou, K.J.,Haralambous, Evaluation of modified mineral performance for chromate sorption from aqueous solutions.Chemical Engineering Journal 211–212, (2012),77–88.

[28] A., Gładysz-Plaska, M., Majdan, S., Pikus, D., Sternik, Simultaneous adsorption of chromium(VI) and phenol on natural red clay modified by HDTMA. Chemical Engineering Journal 179, (2012),140-150.

[29] S., Dultz, J.H., An, B., Riebe, Organic cation exchanged montmorillonite and vermiculite as adsorbents for Cr(VI): Effect of layer charge on adsorption properties. Applied Clay Science 67–68 (2012) 125–133.

[30] M., Majdan, O., Maryuk, S., Pikus, E., Olszewska, R., Kwiatkowski, H., Skrzypek, Equilibrium, FTIR, scanning electron microscopy and small wide angle X-ray scattering

studies of chromates adsorption on modified bentonite. Journal of Molecular Structure, 740,203–211, 2005.

[31] S.,Pandey, S.B.,Mishra, Organic–inorganic hybrid of chitosan/organoclay bionanocomposites for hexavalent chromium uptake. Journal of Colloid and Interface Science, 361, (2011), 509–520.

[32] A.S.K., Kumar, R., Ramachandran, S., Kalidhasan, V., Rajesh, N., Rajeshet, Potential application of dodecylamine modified sodium montmorillonite as an effective adsorbent for hexavalent chromium. Chemical Engineering Journal, 211-212, (2012), 396-405.

[33] I., Daou, R., Chfaira, O., Zegaoui, Z., Aouni, and H., Ahlafi, Mediterranean J. of Chemistry, 2(4), (2013), 570-584.